PROCEEDINGS B

Review

CrossMark
click for updates

Authors for correspondence:
Erik A. Martens
e-mail: erik.martens@ds.mpg.de
Navish Wadhwa
e-mail: nawa@fysik.dtu.dk

†These authors contributed equally to this work.

THE ROYAL SOCIETY
PUBLISHING

Size structures sensory hierarchy in ocean life

Erik A. Martens[1,2,3,†], Navish Wadhwa[1,4,†], Nis S. Jacobsen[1,2], Christian Lindemann[2], Ken H. Andersen[1,2] and André Visser[1,2]

[1]VKR Centre for Ocean Life, and [2]National Institute of Aquatic Resources, Technical University of Denmark, Jægersborg Alle 1, 2920 Charlottenlund, Denmark
[3]Department of Biomedical Sciences, Copenhagen University, Blegdamsvej 3, Copenhagen 2200, Denmark
[4]Department of Physics, Technical University of Denmark, Kongens Lyngby 2800, Denmark

Survival in aquatic environments requires organisms to have effective means of collecting information from their surroundings through various sensing strategies. In this study, we explore how sensing mode and range depend on body size. We find a hierarchy of sensing modes determined by body size. With increasing body size, a larger battery of modes becomes available (chemosensing, mechanosensing, vision, hearing and echolocation, in that order) while the sensing range also increases. This size-dependent hierarchy and the transitions between primary sensory modes are explained on the grounds of limiting factors set by physiology and the physical laws governing signal generation, transmission and reception. We theoretically predict the body size limits for various sensory modes, which align well with size ranges found in literature. The treatise of all ocean life, from unicellular organisms to whales, demonstrates how body size determines available sensing modes, and thereby acts as a major structuring factor of aquatic life.

1. Introduction

The marine pelagic environment is sparsely populated. To survive, organisms must scan volumes of water millions of times their own body volumes per day [1]. While searching is a challenge in itself, there is also the continual risk of predation. The result is a strong evolutionary drive to effectively gather information on the proximity of prey, mates and predators [2]. Here, we examine the means by which this information is gathered by marine pelagic organisms, that is, their sensory ability. In particular, we wish to understand relationships between the size of an organism and the usability of the various types of senses.

Indeed, size is a key parameter to characterize biological processes in marine environments [1,3–6]. A cursory examination indicates at least some size-dependent organization as to which sensory modes organisms use in the marine pelagic environment. For instance, the smallest organisms (e.g. bacteria) depend heavily on chemical signals, while for larger animals (e.g. copepods), sensing of fluid flows becomes important too. For even larger organisms, vision (e.g. crustaceans and fishes), hearing (e.g. fishes) and echolocation (e.g. toothed whales) become increasingly relevant sensory modes (electronic supplementary material, figure S1). How can we understand this pattern on the grounds of physiology and physics using scaling rules, which are the two basic constraints on the workings of any organism [7,8]? Our aim here is to determine the body size limits of different sensing modes based on physical grounds and to explain how the sensory hierarchy is structured by size.

2. Sensing as a physical process

Our goal is to understand how size determines sensory modes available to an organism. We restrict ourselves to those sensory modes that are the primary means of remotely detecting the presence of other organisms: chemosensing of compounds, mechanosensing of flow disturbances provoked by moving animals,
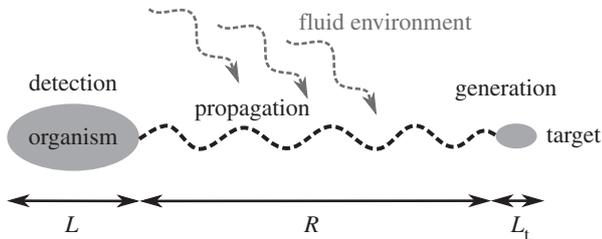
Figure 1. Schematic of the participants and the processes involved in sensing.

image vision in sufficiently lit areas, hearing of sound waves and their generation for echolocation. We further restrict ourselves to the pelagic zone. All sensing involves an organism and a target; thus, we refer to the *organism* of size L and the *target* of size L_t. The two lengths are related via the dimensionless size preference $p = L_t/L$ (we assume $p = 0.1$ for predation, $p = 1$ for mating, $p = 10$ for predator avoidance). Clearly, other modes such as electroreception [9] or magnetoreception [10] may supplement the above-mentioned modes, and organisms may switch between sensing modes depending on proximity to the target; here, however, we restrict ourselves to the aforementioned senses and consider them as the predominant primary sensory modes.

It is possible to decompose sensing into three fundamental sub-processes (figure 1).

(a) Generation

Animals emit signals by creating fluid disturbances, creating sounds or reflecting ambient light. The target's features such as its size, L_t, affect the signal. Chemosensing, hearing and mechanosensing require a signal or an action from the target, whereas vision and echolocation do not. Echolocation in particular is an 'active sense', as the signal is generated by the organism and hence influenced by organism features such as size L.

(b) Propagation

The distance over which a signal propagates before getting subdued by noise is sensitive to many factors. For instance, the oceans are awash with traces of various chemicals. Detection of a specific compound requires concentrations higher than the background and depends on its diffusivity, release rate, stability, etc. This distance sets a sensing range R.

(c) Detection

Is the organism—given the physical constraints—able to build a sensor? This requires a cost-effective mechanism by which information can be collected at a practical level of resolution. Size and complexity of the organism determine this ability.

Each of these sub-processes is constrained by size. Thus, the length scale imprints itself automatically on the remote detection of other organisms. But limits of the usage of specific sensing modes are not necessarily clear-cut. For instance, in case of vision, the boundary between an image-forming eye (e.g. in fishes) and non-image-forming 'eye spots' that enable phototaxis (e.g. in copepods, protists) is not sharply defined. Moreover, simultaneous use of multiple senses complicates the situation. We make the simplifying assumption of no integration between senses, and treat them in isolation from each other. Within its

limitations, this investigation may not yield exact numbers; it provides *characteristic* body-size limits for the sensory modes and yields valuable understanding of the structure of sensing in marine life, based on first principles.

3. Chemosensing

The ability to detect chemical compounds is ubiquitous. All life forms have this ability and are equipped with chemosensing apparatuses [11]. Chemotaxis and the use of chemosensing in remote detection can be divided into two modes: (i) gradient climbing defined as moving along a gradient towards (or away from) a stationary target, and (ii) following a trail laid out by a moving target [12,13].

(a) Size limits for chemosensing

Gradient climbing ability would be size independent, were it not for two randomizing physical effects. For very small organisms, gradient climbing ability is impaired owing to Brownian rotation [14], caused by molecular motions in the fluid. Owing to this, the organism cannot direct itself along a gradient using a biased random walk (figure 2a). This happens for L less than the length-scale characteristic of Brownian motion, L_{Br} (0.1–1 μm) [15]. Using a similar argument, Dusenbery [16] has argued that below $L = 0.6$ μm, directed motility, and thus chemotaxis, is infeasible owing to Brownian rotation.

An upper limit for gradient climbing is imposed when turbulence disrupts the smoothness of the chemical gradient, for L greater than the Batchelor scale $L_B \approx (\nu D^2/\varepsilon)^{1/4}$, where ν is the kinematic viscosity, D the molecular diffusivity and ε the turbulent energy dissipation rate. L_B is the length scale at which the diffusion time scale becomes comparable to the dissipation time for the smallest turbulent eddies (figure 2b). In the ocean, ε ranges between 10^{-8} and 10^{-3} m^2 s^{-3} [17,18]. L_B is between 5 and 100 μm in moderate turbulence (for a typical value of $D \sim 10^{-9}$ m^2 s^{-1}), but can become much larger in quiescent environments.

For detecting a moving target that releases a chemical trail, the physical constraints are similar to gradient climbing. For L above the Kolmogorov scale $L_K \approx (\nu^3/\varepsilon)^{1/4}$, directional information in the trail is reduced owing to the isotropy in turbulent flows [19], impairing chemotaxis. L_K is around 1 cm in moderate turbulence [17], above which trail following becomes progressively worse. When L is larger than the integral length-scale L_I, trail following may become effective again as the turbulent trail at this scale is anisotropic (figure 2c). Typical values for L_I in a stratified ocean are around 1 m or larger [20,21]. Thus, between approximately 1 cm and approximately 1 m, trail following is impaired, and requires averaging over space and time [22]. Note that in the absence of environmental turbulence, L_K and L_I are determined by the size of the trail source.

(b) Sensing range for chemosensing

Size limits for the functioning of chemosensing also apply to the sensing range. For example, in gradient climbing, the maximal distance up to which a chemical gradient remains uninterrupted is L_B. Another factor affecting the range for gradient climbing is the diffusion time scale. For a typical compound to diffuse over $d = 1$ cm, it can take up to days ($t = d^2D^{-1}$, where $D \sim 10^{-9}$ m^2 s^{-1}). This makes the signal irrelevant for many small
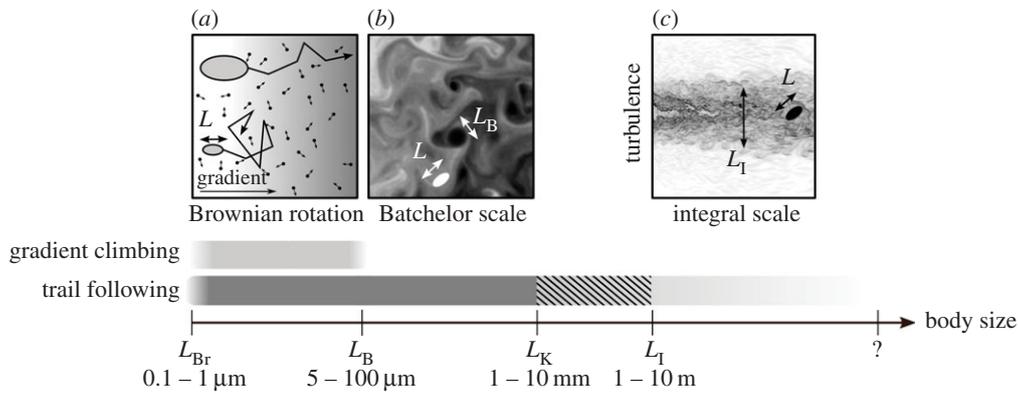
Figure 2. Body sizes over which chemosensing can be used effectively. A schematic illustration of Brownian rotation (*a*), Batchelor scale (*b*), and integral scale (*c*) is included at the top.

organisms, because by that time they have moved elsewhere, been preyed upon or have multiplied several times. Thus, gradient climbing is relevant only up to small distances. Similarly, for trail following, sensing range is limited to L_K.

4. Mechanosensing

Any object moving in fluid generates a hydromechanical disturbance that can potentially be detected with the appropriate sensory apparatus [23]. For many small organisms such as zooplankton [23–25], it is the dominant sensory mechanism. Many fishes, especially in dimly lit environments, also rely heavily on mechanosensing using the lateral line organ [26]. The nature of a fluid disturbance generated by a target of size L_t swimming with a velocity U_t is largely determined by the dimensionless Reynolds number (Re), defined as $Re = L_t U_t / \nu$, where ν is the kinematic viscosity [27]. For small Re, such as for most plankton, flow is dominated by viscosity and is laminar [28]. For large Re, such as for large fishes or mammals, inertia dominates and the flow tends to be turbulent [29].

(a) Propagation of fluid disturbances

For a target passively sinking at low Re in unbounded fluid (e.g. the pelagic zone), the velocity (u) induced in the fluid decays with distance r as $u \sim r^{-1}$ [23]. For a self-propelled target, the induced velocity decays as $u \sim r^{-2}$ [23]. Recent studies have shown that for breast-stroke swimming plankton and impulsively jumping copepods, u decays more rapidly as $u \sim r^{-3}$ and $u \sim r^{-4}$, respectively [30,31]. At high Re, the fluid disturbance generated by a target becomes turbulent, if L_t is much larger than L_K, resulting in a turbulent wake.

(b) Detection

Setae on the antennae of a copepod are classic examples of mechanosensors (electronic supplementary material, figure S2). Setae sense velocity difference across their length, and activate when it exceeds a certain threshold s [25], defining setae sensitivity [32], typically between 10 and 100 μm s^{-1} [23]. In unicellular organisms such as ciliates and dinoflagellates, a response occurs above a critical fluid deformation rate [24,33], equivalent to a threshold velocity difference across the cell. In the lateral lines of fishes, the working sensor is a seta-like kinocilium [34]. In general, mechanosensing requires a velocity differential on the organism's body, as a result of

fluid deformation. Given a sensitivity s of a mechanosensor of length b, embedded in fluid with deformation rate Δ (measured in s^{-1}), the criterion for detection can be written as

$$\Delta \cdot b > s. \tag{4.1}$$

(c) Sensing range for mechanosensing

We estimate the sensing range R for the most relevant case of a self-propelled target. For $R \gg b$, Visser [23] has shown that $R \approx (3 U_t L_t^2 b / s)^{1/3}$. The swimming velocity of the target is related to its size by the empirical relation $U_t \sim c_1 L_t^{0.79}$ with $c_1 = 6.5$ m$^{0.21}$ s^{-1} [1]. For prey detection ($p = 0.1$), assuming that the sensor is about a tenth of the body size ($b = L/10$), we get

$$R \approx c_2 L^{1.26}, \tag{4.2}$$

where $c_2 = 3.98$ m$^{-0.26}$.

From this estimate, a copepod of $L \sim 2$ mm has a prey sensing range of about 1.5 mm. The exact scaling coefficient is determined by the organism's morphology and the swimming characteristics of the target, but equation (4.2) provides a rough estimate. Like in chemical trail following, an upper limit of mechanosensing range R is set by the Kolmogorov scale, L_K, above which turbulence disrupts the signal.

(d) Size limits for mechanosensing

The lower size limit for mechanosensing in the pelagic zone is dictated by inequality (4.1). We consider the case of a small prey individual detecting a larger predator ($p = 10$). For a target (predator) swimming with a velocity U_t, fluid deformation scales as $\Delta \sim U_t / L_t$. Using again the empirical scaling of $U_t \sim c_1 L_t^{0.79}$ [1], and further using $L = L_t / 10$, we can deduce that

$$\Delta \sim c_3 \cdot L^{-0.21}, \tag{4.3}$$

where $c_3 = 3.98$ m$^{0.21}$ s^{-1}.

To close the problem, we again use $b = L/10$. Combining equations (4.1) and (4.3), substituting b and using an intermediate value for $s = 50$ μm s^{-1}, we get a lower size limit of $L > 11$ μm. Thus we expect the lower size limit for an organism to use mechanosensing in the pelagic zone to be of the order of a few micrometres. Given the sensitivity of mechanosensing apparatuses, smaller organisms are unable to detect the hydromechanical disturbances relevant to their size.

The upper size limit of mechanosensing is prescribed by the same constraints as those for chemical trail following.

The generated flows are disintegrated by turbulence at $L > L_K$, rendering mechanosensing progressively less effective above organism sizes of around 1 cm. We also conjecture that like trail following, mechanosensing abilities may improve for organisms larger than the integral length-scale L_I.

5. Vision

Simple functions of vision include differentiating light from dark, entrainment to a circadian rhythm [35], and orientation [36], while more complex functions involve navigation, pattern recognition and food acquisition. Prey and predator detection from some distance requires sufficient image resolution. In general, only two fundamental principles are used to build an eye: (i) compound eyes, which comprises a number of individual lenses and photo-receptors laid out on a convex hemispherical surface, and (ii) camera eyes with one concave photoreceptive surface where an image is projected through an optical unit (pinhole or lens).

(a) Light propagation in the marine environment

Given that a target is lit and visible, the reflected light must travel through seawater to reach the receiving organism. The intensity of light attenuates geometrically with distance r as r^{-2}, and more steeply owing to the added effects of scattering and absorption by solutes and seston [37]. In general, light intensity along a given path decreases as $e^{-\alpha r}$, where α (measured in m^{-1}) is called the absorption coefficient [38].

(b) Physiological limits to eye size

The resolution of the compound eye is limited by the size of ommatidia (photoreceptor units in compound eyes). They cannot be reduced in size to achieve a resolution better than $1°$ [39]. Thus, camera eyes, which we consider in the following, outperform compound eyes in compactness [39,40]. The functioning of a small eye is limited by two constraints. First, a smaller eye captures less light. Second, a smaller eye has lower resolution: the photoreceptive units constitute the smallest components in an eye and are based on opsin molecules, the universally represented light-capturing design in the animal world [41]. Thus, the width of a photoreceptor $d_p \approx 1\,\mu m$ [42] is an absolute limiting factor for any eye design. Therefore, n pixels amount to a retina diameter of $d \approx n^{1/2} d_p$. Considering a minimal required resolution for a usable image-forming eye to be 100^2 pixels, the corresponding retina would have a diameter $d \approx 0.1$ mm. Depending on the eye-to-body size ratio, this corresponds to an organism of around $L \approx 1$–3 mm.

Arguments for an upper size limit for eyes are not evident on physical grounds. The largest known marine animals carry eyes (see Discussion). However, the higher resolution and sensitivity resulting from larger eyes do not necessarily yield a larger sensing range as it may be limited by turbidity, as we discuss next.

(c) Visual range

The visual range of an organism can be estimated by considering the properties of a (pinhole) camera eye, following an argument by Dunbrack & Ware [43]. We use Weber contrast $C = (I - I_b)/I_b$, where I and I_b are the intensities of the target and the background, respectively. The maximal distance R at

which a predator can discern a prey individual of size L_t requires that the apparent contrast C_a of the target matches the contrast threshold of the eye, C_{th}. The inherent contrast of the target, C_0 declines with distance r, yielding [38]

$$C_a = C_0 \cdot e^{-\alpha r}. \tag{5.1}$$

C_{th} is a declining function of the number of visual elements n involved in perceiving the target:

$$C_{th} = C_{th,\,min}(z) + \frac{K_{ph}}{n}. \tag{5.2}$$

This formula is partly based on Ricco's law [44] that expresses the inverse proportionality between C_{th} and n, and is supplemented by adding the minimum contrast threshold $C_{th,min}$ to represent saturation of the contrast at a minimal value [45]. $C_{th,min}$ varies in different environments and, in particular, depends on the available backlight at a given depth z.

The number of visual elements n involved in image detection is equal to their density, σ (measured in m^{-2}), times the projected image area. Assuming R is large relative to the eye ball diameter L_{eye}, we can deduce $n = \sigma \pi / 4 L_{img}^2 \approx \sigma L_{eye}^2 L_t^2 R^{-2}$ (electronic supplementary material, figure S3). Noting the universal size of the opsin molecule across species, we may assume that σ is independent of eye size. Introducing the ratio $a = L_{eye}/L$ [46] and using $p = L_t/L$, we get $n = \sigma a^2 p^2 L^4 R^{-2}$. The range R is determined by the condition $C_a \geq C_{th}$:

$$C_0 e^{-\alpha R} \geq C_{th,\,min}(z) + KR^2 L^{-4}, \tag{5.3}$$

where $K = K_{ph} \sigma^{-1} a^{-2} p^{-2}$ is a constant characterizing the photoreceptor sensitivity, K_{ph}/σ, eye-to-body-size ratio, a, and size preference, p. Sample solutions for the condition $C_a = C_{th}$ yield the range R at a given body size L (figure 3a). Isolating R from equation (5.3) is impossible; however, asymptotic solutions can be derived for two limits:

(i) 'clear-water limit': when $\alpha \to 0$, R is limited by the eye's resolution; thus, $R \sim [(C_0 - C_{th,\,min})/K]^{1/2} L^2$; and
(ii) 'turbid-water limit': when $C_0 - C_{th,\,min} \gg KR^2 L^{-4}$; thus, $R \sim (\ln C_0 - \ln C_{th,min})/\alpha$. R is independent of L and only limited by the sensitivity of a visual element, $C_{th,min}$.

Generally, the visual range decreases if light is reduced, e.g. at large depth z, leading to a higher $C_{th,min}$ (cases (i) and (ii)); or if the turbidity is strong (larger α) (case (ii)). The cross-over between the two limits occurs when $L \sim L_x \sim \alpha^{-1/2}$ (electronic supplementary material). The visibility range in pure water for light of 550 nm is theoretically estimated at 74 m [48], and measurements in the open sea range from 44 to 80 m [49]. The visual range has also been predicted in more elaborate models [50].

6. Hearing

Sound propagates through the ocean as pressure waves, resulting in alternating compression and rarefaction of water in regions of high and low pressure, respectively. Any form of hearing must detect sound waves by converting them into vibrations of an organ that stimulates nerve cells. In fishes, sound waves displace sensory hairs against the calcareous
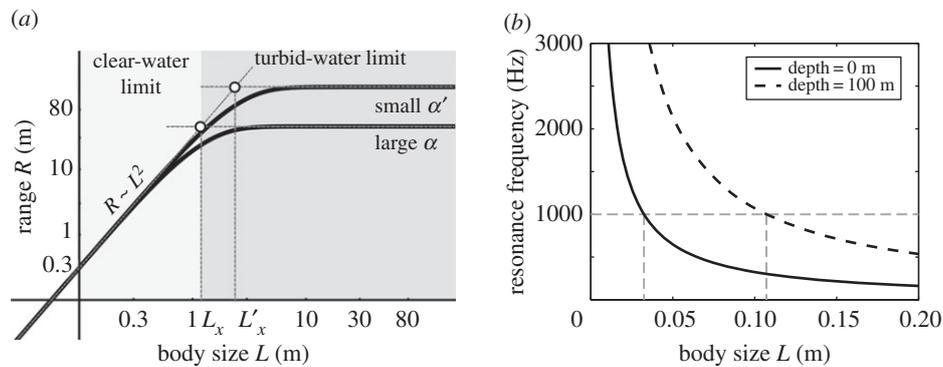
Figure 3. (a) Visual sensing range scales with body size, L, as $R \sim L^2$ in the clear-water limit ($L \ll L_x$) and as $R \sim$ constant in the turbid-water limit ($L \gg L_x$). Parameters are $C_0 = 0.3$, $C_{th,min} = 0.05$ (adopted from [43]), $K = 2.5 \times 10^{-4} \text{ m}^2$, $\alpha = 0.04 \text{ m}^{-1}$ [47] (and $\alpha' = 0.01 \text{ m}^{-1}$ for comparison). (b) Relationship of body size and resonance frequency based on equation (6.1) and using a swim bladder size $r_b = L/10$ for an individual at the surface (solid curve) and at 100 m depth (dashed curve). The dashed (grey) horizontal line indicates 1 kHz, below which most sounds generated by marine life are found.

otolith, and this relative motion is detected. By contrast, in mammalian ears, sound waves excite the tympanic membrane (eardrum), the motion of which is sensed by ciliary hairs in the cochlea.

Most sounds relevant to ocean life, except echolocation, fall into the range of a few hertz up to a few kilohertz. Sounds generated by marine animals owing to rapid movements or for communication, have frequencies rarely exceeding 1 kHz [51]. Communication by marine mammals usually consists of a burst of clicks or of whistles (4–12 kHz), while the echolocating signals of odontoceti range between 20 and 200 kHz [52].

(a) Underwater sound propagation
As sound waves travel through a medium, sound intensity attenuates with distance from the target r, owing to two processes: (i) geometric spreading (r^{-2} in open space) and (ii) absorption in water. The latter is frequency dependent: 1 dB km^{-1} at 10 kHz, but only 10^{-4} dB km^{-1} at 100 Hz in seawater [38].[1] Sound is therefore only weakly attenuated in seawater, and it can potentially carry information over large distances.

(b) Lower limit for sound detection
Detection of sound requires either an organ of significantly different density than that of water (e.g. the otolith), or a large detector array (e.g. auricle and drum), to allow detection by responding to spatial gradients of particle displacement [38]. A density contrast organ such as the otolith has to move relative to the surrounding fluid, as explained above. Motions in small sound-sensing organs (operating at low Re) are inherently more damped by viscosity than larger ones, impairing the practicality of sound detection by small organisms. Without high-density contrast in the hearing organ, the detector array and thus the organism would have to be at least as long as the wavelength of sound (15 cm at 10 kHz). Thus hearing—with or without a density contrast organ—is impractical for pelagic organisms smaller than a few centimetres.

Many fishes have swim bladders (sometimes connected to the otolith-containing cavity through bony connections called the *Weberian ossicles*) that transduce pressure waves to mechanical motion and act as displacement amplifiers for sound via resonance [38,53]. Similarly, odontocetes use the fat-filled bones of their lower jaw as an amplifying cavity [52]. Swim bladders are air-filled structures that

amplify sound maximally when in natural resonance with the sound waves [38]. Frequencies very different from the resonance frequency of the swim bladder do not amplify well, and may even be damped if too different [38]. Based on an assumption of a spherical, air-filled swim bladder, the resonance frequency, f, can be approximated [38] as

$$f = \frac{1}{2\pi r_b} \sqrt{\frac{3\Gamma P}{\rho}}, \tag{6.1}$$

where P is the depth-dependent hydrostatic pressure, r_b the radius of the swim bladder, ρ the density of seawater and Γ the adiabatic exponent (approx. 1.4 for air); r_b is typically around 5–10% [54] of the body size L of the fish. Using $r_b = L/10$ for a conservative estimate, L would need to be at least 3 cm at the sea surface, in order to amplify the high-frequency end (1 kHz) of the ambient underwater sound spectrum, and $L = 11$ cm at a depth of 100 m (figure 3b). To hear the more typical lower frequencies, L would have to be larger still. Thus, we approximate that the lower body size limit for detection of sound using swim bladders is around a few centimetres.

7. Echolocation
Echolocation is an active sensing mode, in which the organism emits clicks in the ultrasonic range and interprets the environment based on the echoes of these clicks. Echolocation is common in odontocetes (toothed whales) and is generally used for orientation and prey detection. The generation of echolocating signals in toothed whales is associated with the nasal passage leading up to the blowhole and takes place in the phonic lips. Taking into account the anatomical structures, the dominant frequency can be estimated as the resonance frequency of a Helmholtz oscillator [55]. The diffraction limit sets a resolution limit to $\lambda/2\pi$, where λ is the characteristic wavelength of the click [38]. Odontocetes produce clicks with peak energies at frequencies in the range of 20–200 kHz [52], the resulting resolution lies between 1 and 8 mm. Using an intermediate value (5 mm), and assuming that the target is at least one order of magnitude larger than the smallest resolvable feature, we get a minimal target size of 50 mm. Echolocation is typically used for prey detection, so $p = 0.1$. Thus we get a lower body size limit for an echolocating organism to be $L \approx 500$ mm. It also implies that objects smaller than about 1 mm do not scatter
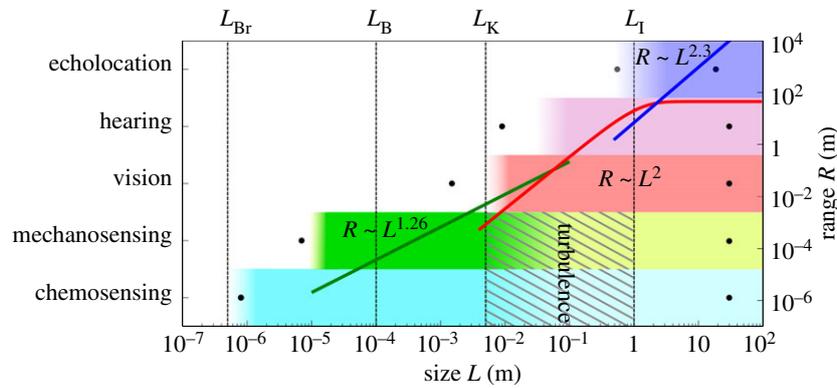
Figure 4. Upper and lower body size limits and ranges for different senses. Dots denote the largest and smallest sizes known to employ a given sense, and shaded rectangles show the theoretical estimates of the size range in which a sense is expected to work. Green, red and blue curves show the theoretical scaling of sensing range with size for mechanosensing, vision and echolocation, respectively.

Table 1. Lower and upper size (body length) limits for various senses. (Predicted theoretical limits denote orders of magnitude.)

	observed limit		theoretical limit	
	lower (m)	upper (m)	lower (m)	upper (m)
chemosensing	8×10^{-7} [16]	30 [56]	$\sim 10^{-7}$	—
mechanosensing	7×10^{-6} [57]	30 [56]	$\sim 10^{-5}$	—
vision	1.5×10^{-3} [58]	30 [56]	$\sim 10^{-3}$	—
hearing	9×10^{-3} [59]	30 [56]	$\sim 3 \times 10^{-2}$	—
echolocation	0.55 [60]	18.6 [61]	~ 0.5	—

sound signals in the frequency range we are considering, allowing echolocation to be useful in turbid waters where vision is severely restricted.

(a) Sensing range

The generated acoustic signal first travels through water, is then partially reflected by the target, and the remainder of the signal (minus attenuation) travels back to the organism. Emitted sound intensity, I_e, is thus reduced by the processes of reflection and geometric divergence, causing signal intensity to attenuate as $(2r)^{-2}e^{-2\mu r}$. The strength of the returned signal must exceed the threshold intensity for detection in the ear, $I_r = I_0$. Assuming that ear threshold sensitivity is independent of L, but that emitted sound intensity I_e and carrier frequency scale with L, the sensing range can be estimated as (electronic supplementary material for details)

$$R \sim pI_0^{-1/2}L^{\gamma}, \tag{6.2}$$

where $p = L_t/L$ is the size preference ratio and the exponent γ lies between 2.125 and 2.5 that compares reasonably well with data. The scaling factor can be estimated from data describing the echolocation range of small marine mammals (electronic supplementary material).

8. Discussion

We have attempted to synthesize an understanding of how physiology and the physical environment enable and constrain an aquatic organism's ability to gather information from its surroundings. By reducing the relevant physical mechanisms to their simplest forms, we have identified the

most pressing constraints on the functioning of various senses. Our goal has been to explain the transition from one dominant sense to another with changing body size, as observed in nature. A comparison of the predicted size limits with those observed in nature supports our analysis (table 1 and figure 4). The predicted size ranges correspond well with known minimal and maximal sizes of animals using a specific sense. Size limits of a sense do not imply that an organism cannot detect the signal outside the limits at all, but rather that beyond these limits, the usefulness of the sense is compromised in comparison with other senses.

We could not conceive any upper size limits on physical grounds for chemosensing, mechanosensing, hearing and vision. Indeed, the largest known organism in the ocean, the blue whale ($L = 30$ m), is known to use all of these senses. Chemosensing is the only sense available to the smallest organisms, and its theoretical lower size limit ($L_{Br} \sim 10^{-7}-10^{-6}$ m) is consistent with the smallest known motile organisms (bacteria, $L = 0.8 \, \mu$m [16]). Chemosensing is presumably slightly impaired owing to turbulence in intermediate size ranges, in which integration of multiple senses such as mechanosensing and vision might be very useful. Chemosensing for trail following is an important sensory mode for large bony fishes [62] and sharks [63], which have sizes larger than L_I.

The theoretical lower limit for mechanosensing in the pelagic environment is a few micrometres, in the realm of protists; to our knowledge, marine protists sized $7-10 \, \mu$m are the smallest pelagic organisms known to use mechanosensing [57]. However, it is only the lower limit for pelagic zones; smaller bacteria are known to be able to sense mechanical stresses when in contact with a solid body [64]. Large copepods and small fishes occupy the size range where mechanosensing starts becoming less effective. Its use by

fishes is demonstrated in many species using lateral lines to find prey and sense flows [26]. Larger fishes receive a poorer signal quality owing to turbulence, and for this reason some larger sharks are known not to use lateral lines for prey detection [65]. Some marine mammals (seals and sea lions) have the ability to follow turbulent trails using their mystacial vibrissae [66], probably owing to being larger than the integral length scale set by the target.

The camera eye takes records for both the smallest and the largest eye: the smallest image-forming eyes (and body sizes) are found in the fish *Schindleria brevipinguis* ($L \approx$ 7 mm [67]), and the pygmy squids ($L \approx 1.5$ mm [58]), which compares well with our predicted size limit.[2] The largest known eye belongs to the giant squid, featuring eyeballs up to 30 cm in diameter [68]. Eyes are also found in the largest known species (whales), implying that there is no upper body size limit for image-forming vision in marine animals.

For hearing, the theoretical lower body size limit is found to be a few centimetres. Some fishes are able to manipulate the resonance frequency of swim bladders by changing their membrane elasticities [69]. By hearing outside the resonance frequency, fish larvae of a few millimetres ($L \approx 9$ mm) have been shown to react to sounds [59]. Note that these fishes inhabit shallower waters, where hearing is feasible at smaller sizes (figure 3*b*). For echolocation, the predicted lower limit (approx. 0.5 m) is close to the observed smallest size among echolocating marine mammals (Commerson's dolphin [60]).

Upper limits of sensing ranges are dictated by degradation of signal-to-noise ratios via absorption, geometric spreading (divergence) or environmental disturbances. For chemical gradient climbing and mechanosensing, the signals are randomized beyond a characteristic distance given by L_B and L_K, respectively. For mechanosensing, the range scales as $R \sim L^{1.26}$ (figure 4). When mechanosensing can no longer extend its range, vision becomes a viable solution. Visual sensing range in clear water scales as $R \sim L^2$, but cannot exceed the limit set by turbidity. Even in clear waters, vision cannot exceed the range of roughly 80 m. Here, vision may be complemented by hearing and echolocation mainly because sound is capable of travelling large distances in seawater without significant attenuation. Although we could not develop a scaling for hearing range, we could determine the sensing range of echolocation, which scales approximately as $R \sim L^{2.3}$ and is as large as kilometres for larger organisms, comparing well with the known range of marine mammals.

The question arises whether there is a general pattern underlying the size structure of primary sensory modes. For instance, can the transitions between senses be related to metabolic demand? Kleiber's law requires that an organism consumes energy at a rate proportional to $L^{9/4}$ [3]. This demand must be fulfilled by maintaining a sufficient clearance rate [4], a function of the swimming velocity $V \sim L^x$ and sensing range $R \sim L^y$ with positive exponents x, y. Thus, the clearance rate also increases with L. The exponent y appears to increase going up the senses axis (figure 4). With increasing size and metabolic expenditure, an evolutionary pressure arises to extend the sensing range by investing into a more effective sensory strategy, causing the transition from one to the other primary sensing mode. However, rather than being governed by cost efficiency, it seems more plausible that the transitions between senses are set by the physical limitations of signal generation, transmission and reception. To exemplify, carrying larger eyes can improve resolution and thus extend the sensing range, but beyond a critical (eye) size, increased performance is rendered ineffective owing to the clear-water limit of the visual range. So a transition is necessitated by the required increase in sensing range, achieved by echolocation.

We have combined biological knowledge, physiology and physics to describe the abilities of the sensory modes in ocean life, from bacteria to whales. Our treatise demonstrates how body size determines available sensing modes, and thereby acts as a major structuring factor of aquatic life. When interpreting the scalings and limits we propose, note that our purpose is to provide first-order approximations based on first principles. Further research is needed to evaluate each of the senses in more detail and to gather more data to examine the arguments presented here. We hope that this work may serve as a starting point for future explorations on sensory modalities and their hierarchical structures.

Endnotes

[1] The decibel level is defined via $I_{dB} = 10 \log_{10}(I/I_0)$, where I is the sound intensity and I_0 is a reference frequency.

[2] The smallest compound eyes are found in the genus *Daphnia*, but their image quality is questionable (see the electronic supplementary material).

References

1. Kiørboe T. 2011 How zooplankton feed: mechanisms, traits and trade-offs. *Biol. Rev.* **86**, 311–339. (doi:10.1111/j.1469-185X.2010.00148.x)

2. Dusenbery DB. 1992 *Sensory ecology: how organisms acquire and respond to information.* New York, NY: WH Freeman.

3. Kleiber M. 1932 Body size and metabolism. *Hilgardia* **6**, 315–351. (doi:10.3733/hilg.v06n11p315)

4. Andersen KH, Beyer JE. 2006 Asymptotic size determines species abundance in the marine size spectrum. *Am. Nat.* **168**, 54–61. (doi:10.1086/504849)

5. Andersen KH et al. 2016 Characteristic sizes of life in the oceans, from bacteria to whales. *Annu. Rev. Mar. Sci.* **8**, 125. (doi:10.1146/annurev-marine-122414-034144)

6. Dusenbery DB, Snell TW. 1995 A critical body size for use of pheromones in mate location. *J. Chem. Ecol.* **21**, 427–438. (doi:10.1007/BF02036740)

7. Dusenbery DB. 2001 Physical constraints in sensory ecology. In *Ecology of sensing* (eds FG Barth, A Schmid), pp. 1–17. Berlin, Germany: Springer.

8. Dusenbery DB. 2009 *Living at micro scale: the unexpected physics of being small*. Cambridge, MA: Harvard University Press.

9. Collin SP, Whitehead D. 2004 The functional roles of passive electroreception in non-electric fishes. *Anim. Biol.* **54**, 1–25. (doi:10.1163/1570756 04323010024)

10. Johnsen S, Lohmann KJ. 2005 The physics and neurobiology of magnetoreception. *Nat. Rev. Neurosci.* **6**, 703–712. (doi:10.1038/nrn1745)

11. Adler J. 1966 Chemotaxis in bacteria. *Science* **153**, 708–716. (doi:10.1126/science.153.3737.708)

12. Moore PA, Fields DM, Yen J. 1999 Physical constraints of chemoreception in foraging copepods. *Limnol. Oceanogr.* **44**, 166–177. (doi:10.4319/lo.1999.44.1.0166)

13. Andrews JC. 1983 Deformation of the active space in the low Reynolds number feeding current of calanoid copepods. *Can. J. Fish. Aquat. Sci.* **40**, 1293–1302. (doi:10.1139/f83-147)

14. Berg HC. 1988 A physicist looks at bacterial chemotaxis. *Cold Spring Harb. Symp. Quant. Biol.* **53**, 1–9. (doi:10.1101/SQB.1988.053.01.003)

15. Mitchell JG. 1991 The influence of cell size on marine bacterial motility and energetics. *Microb. Ecol.* **22**, 227–238. (doi:10.1007/BF02540225)

16. Dusenbery DB. 1997 Minimum size limit for useful locomotion by free-swimming microbes. *Proc. Natl Acad. Sci. USA* **94**, 10 949–10 954. (doi:10.1073/pnas.94.20.10949)

17. Jiménez J. 1997 Oceanic turbulence at millimeter scales. *Sci. Mar.* **61**, 47–56.

18. Visser AW, Saito H, Saiz E, Kiørboe T. 2001 Observations of copepod feeding and vertical distribution under natural turbulent conditions in the North Sea. *Mar. Biol.* **138**, 1011–1019. (doi:10.1007/s002270000520)

19. Tennekes H, Lumley JL. 1972 *A first course in turbulence*. Cambridge, MA: MIT Press.

20. Yamazaki H, Mackas DL, Denman KL. 2002 Coupling small-scale physical processes with biology. *Sea* **12**, 51–112.

21. Visser AW. 1997 *Small, wet & rational: individual based zooplankton ecology*. Kongens Lyngby, Denmark: Technical University of Denmark.

22. Vergassola M, Villermaux E, Shraiman BI. 2007 'Infotaxis' as a strategy for searching without gradients. *Nature* **445**, 406–409. (doi:10.1038/nature05464)

23. Visser AW. 2004 Hydromechanical signals in the plankton. *Mar. Ecol. Prog. Ser.* **222**, 1–24. (doi:10.3354/meps222001)

24. Jakobsen HH. 2001 Escape response of planktonic protists to fluid mechanical signals. *Mar. Ecol. Prog. Ser.* **214**, 67–78. (doi:10.3354/meps214067)

25. Yen J, Lenz PH, Gassie DV, Hartline DK. 1992 Mechanoreception in marine copepods: electrophysiological studies on the first antennae. *J. Plankton Res.* **14**, 495–512. (doi:10.1093/plankt/14.4.495)

26. Montgomery JC. 1989 Lateral line detection of planktonic prey. In *The mechanosensory lateral line* (eds S Coombs, P Görner, H Münz), pp. 561–574. New York, NY: Springer.

27. Pozrikidis C. 2011 *Introduction to theoretical and computational fluid dynamics*, 2nd edn. Oxford, UK: Oxford University Press.

28. Lauga E, Powers TR. 2009 The hydrodynamics of swimming microorganisms. *Rep. Prog. Phys.* **72**, 096601. (doi:10.1088/0034-4885/72/9/096601)

29. Batchelor GK. 1967 *An introduction to fluid dynamics*. Cambridge, UK: Cambridge University Press.

30. Jiang H, Kiørboe T. 2011 The fluid dynamics of swimming by jumping in copepods. *J. R. Soc. Interface* **8**, 1090–1103. (doi:10.1098/rsif.2010.0481)

31. Kiørboe T, Jiang H, Gonçalves RJ, Nielsen LT, Wadhwa N. 2014 Flow disturbances generated by feeding and swimming zooplankton. *Proc. Natl Acad. Sci. USA* **111**, 11 738–11 743. (doi:10.1073/pnas.1405260111)

32. Kiørboe T, Visser A. 1999 Predator and prey perception in copepods due to hydromechanical signals. *Mar. Ecol. Prog. Ser.* **179**, 81–95. (doi:10.3354/meps179081)

33. Maldonado EM, Latz MI. 2007 Shear-stress dependence of dinoflagellate bioluminescence. *Biol. Bull.* **212**, 242–249. (doi:10.2307/25066606)

34. Bleckmann H. 1986 Role of the lateral line in fish behaviour. In *The behaviour of teleost fishes* (ed. TJ Pitcher), pp. 177–202. New York, NY: Springer.

35. Kreimer G. 2009 The green algal eyespot apparatus: a primordial visual system and more? *Curr. Genet.* **55**, 19–43. (doi:10.1007/s00294-008-0224-8)

36. Jékely G, Colombelli J, Hausen H, Guy K, Stelzer E, Nédélec F, Arendt D. 2008 Mechanism of phototaxis in marine zooplankton. *Nature* **456**, 395–399. (doi:10.1038/nature07590)

37. Wozniak B, Dera J. 2007 *Light absorption in sea water*. New York, NY: Springer.

38. Denny MW. 1993 *Air and water: the biology and physics of life's media*. Princeton, NJ: Princeton University Press.

39. Land MF. 1997 Visual acuity in insects. *Annu. Rev. Entomol.* **42**, 147–177. (doi:10.1146/annurev.ento.42.1.147)

40. Barlow HB. 1952 The size of ommatidia in apposition eyes. *J. Exp. Biol.* **29**, 667–674.

41. Land MF, Fernald RD. 1992 The evolution of eyes. *Annu. Rev. Neurosci.* **15**, 1–29. (doi:10.1146/annurev.ne.15.030192.000245)

42. Kolb H. 2014 Part II: anatomy and physiology of the retina: photoreceptors. In *WEBVISION: the organization of the retina and visual system* (eds H Kolb, E Fernandez, R Nelson). Salt Lake City, UT: University of Utah Health Sciences Center.

43. Dunbrack RL, Ware DM. 1987 Energy constraints and reproductive trade-offs determining body size in fishes. In *Evolutionary physiological ecology* (ed. P Calow), pp. 191–218. Cambridge, UK: Cambridge University Press.

44. Schwartz S. 2004 *Visual perception: a clinical orientation*, 3rd edn. New York, NY: McGraw-Hill Professional.

45. Northmore D, Volkmann FC, Yager D. 1978 Vision in fishes: colour and pattern. In *The behavior of fish and other aquatic animals* (ed. DI Mostofsky), pp. 79–136. New York, NY: Academic Press.

46. Howland HC, Merola S, Basarab JR. 2004 The allometry and scaling of the size of vertebrate eyes. *Vis. Res.* **44**, 2043–2065. (doi:10.1016/j.visres.2004.03.023)

47. Beckmann A, Hense I. 2007 Beneath the surface: characteristics of oceanic ecosystems under weak mixing conditions: a theoretical investigation. *Prog. Oceanogr.* **75**, 771–796. (doi:10.1016/j.pocean.2007.09.002)

48. Smith RC, Baker KS. 1981 Optical properties of the clearest natural waters (200–800 nm). *Appl. Opt.* **20**, 177–184. (doi:10.1364/AO.20.000177)

49. DaviesColley RJ, Smith DG. 1995 Optically pure waters in Waikoropupu ('Pupu') Springs, Nelson, New Zealand. *NZ J. Mar. Freshw. Res.* **29**, 251–256. (doi:10.1080/00288330.1995.9516658)

50. Aksnes DL, Giske J. 1993 A theoretical model of aquatic visual feeding. *Ecol. Model.* **67**, 233–250. (doi:10.1016/0304-3800(93)90007-F)

51. Kasumyan AO. 2008 Sounds and sound production in fishes. *J. Ichthyol.* **48**, 981–1030. (doi:10.1134/S0032945208110039)

52. Ketten DR. 1992 The marine mammal ear: specializations for aquatic audition and echolocation. In *The evolutionary biology of hearing* (eds D Webster, RR Fay, AN Popper), pp. 717–750. New York, NY: Springer-Verlag. (doi:10.1007/978-1-4612-2784-7_44)

53. Hawkins AD. 1986 Underwater sound and fish behavior. In *The behaviour of teleost fishes* (ed. TJ Pitcher), pp. 114–151. New York, NY: Springer.

54. Blaxter JHS. 1981 The swimbladder and hearing. In *Hearing and sound communication in fishes* (eds WN Tavolga, AN Popper, RR Fay), pp. 61–71. New York, NY: Springer.

55. Aroyan JL, McDonald MA, Webb SC, Hildebrand JA, Clark D, Laitman JT, Reidenberg JS. 2000 Acoustic models of sound production and propagation. In *Hearing by whales and dolphins* (eds WWL Au, AN Popper, RR Fay), pp. 409–469. New York, NY: Springer.

56. Lockyer C. 1976 Body weights of some species of large whales. *J. Cons.* **36**, 259–273. (doi:10.1093/icesjms/36.3.259)

57. Jakobsen HH, Everett LM, Strom SL. 2006 Hydromechanical signaling between the ciliate mesodinium pulex and motile protist prey. *Aquat. Microb. Ecol.* **44**, 197–206. (doi:10.3354/ame044197)

58. Reid A. 2005 Family idiosepiidae. In *Cephalopods of the world: an annotated and illustrated catalogue of cephalopod species known to date*, no. 4, vol. I (eds P Jereb, CFE Roper), pp. 208–210. Rome, Italy: FAO.

59. Wright KJ, Higgs DM, Leis JM. 2011 Ontogenetic and interspecific variation in hearing ability in marine fish larvae. *Mar. Ecol. Prog. Ser.* **424**, 1–13. (doi:10.3354/meps09004)

8

rspb.royalsocietypublishing.org *Proc. R. Soc. B* **282**: 20151346

9

rspb.royalsocietypublishing.org Proc. R. Soc. B 282: 20151346

60. Joseph BE, Antrim JE, Cornell LH. 1987 Commerson's dolphin (*Cephalorhynchus commersonii*): a discussion of the first live birth within a marine zoological park. *Zool. Biol.* **77**, 69–77. (doi:10.1002/zoo.1430060108)

61. Watwood SL, Miller PJO, Johnson M, Madsen PT, Tyack PL. 2006 Deep-diving foraging behaviour of sperm whales (*Physeter macrocephalus*). *J. Anim. Ecol.* **75**, 814–825. (doi:10.1111/j.1365-2656.2006.01101.x)

62. Løkkeborg S. 1998 Feeding behaviour of cod, *Gadus morhua*: activity rhythm and chemically mediated food search. *Anim. Behav.* **56**, 371–378. (doi:10. 1006/anbe.1998.0772)

63. Hueter RE, Mann DA, Maruska KP, Sisneros JA, Demski LS. 2004 Sensory biology of elasmobranchs. In *Biology of sharks and their relatives* (eds JC Carrier, JA Musick, MR Heithaus), pp. 326–368. Boca Raton, FL: CRC Press.

64. Aprikian P *et al.* 2011 The bacterial fimbrial tip acts as a mechanical force sensor. *PLoS Biol.* **9**, e1000617. (doi:10.1371/journal.pbio.1000617)

65. Gardiner JM, Atema J. 2014 Flow sensing in sharks: lateral line contributions to navigation and prey capture. In *Flow sensing in air and water* (eds H Bleckmann, J Mogdans, SL Coombs), pp. 127–146. Berlin, Germany: Springer.

66. Hanke W, Wieskotten S, Niesterok B, Miersch L, Witte M, Brede M, Leder A, Dehnhardt G. 2012 Hydrodynamic perception in pinnipeds. In *Nature-inspired fluid mechanics, volume 119 of notes on numerical fluid mechanics and multidisciplinary design* (eds C Tropea, H Bleckmann), pp. 255–270. Berlin, Germany: Springer.

67. Watson W, Walker Jr HJ. 2004 The world's smallest vertebrate, *Schindleria brevipinguis*, a new paedomorphic species in the family schindleriidae (Perciformes: Gobioidei). *Rec. Australian Mus.* **56**, 139–142. (doi:10.3853/j.0067-1975.56.2004.1429)

68. Land MF, Nilsson DE. 2002 *Animal eyes*. Oxford, UK: Oxford University Press.

69. Feuillade C, Nero RW. 1998 A viscous-elastic swimbladder model for describing enhanced-frequency resonance scattering from fish. *J. Acoust. Soc. Am.* **103**, 3245–3255. (doi:10.1121/1.423076)